Photoacoustic measurement with infrared band-pass filters significantly overestimate NH_3 emissions from cattle houses due to VOCs interferences

Dezhao Liu[1,2*], Li Rong[2], Jesper Kamp[2], Xianwang Kong[1], Anders Peter S. Adamsen[3], Albarune Chowdhury[2], Anders Feilberg[2*]

1- Zhejiang University, College of Biosystems Engineering and Food Science, Yuhangtang Road 866, 310058 Hangzhou, China

2- Aarhus University, Department of Engineering, Finlandsgade 22, 8200 Aarhus N, Denmark

3- APSA, c/o Agro Business Park, Niels Pedersens Allé 2, DK-8830 Tjele, Denmark

Corresponding author: Dezhao Liu: dezhaoliu@zju.edu.cn;

Anders Feilberg: af@eng.au.dk

Abstract: Infrared photoacoustic spectroscopy using band-pass filters (PAS) is a widely used method for measurement of NH_3 and greenhouse gas emissions (CH_4, N_2O and CO_2) especially in agriculture, but non-targeted gases such as volatile organic compounds (VOCs) from cattle barns may interfere with target gases causing inaccurate results. This study made an estimation of NH_3 interference in PAS caused by selected non-targeted VOCs which were simultaneously measured by a PAS and a PTR-MS (proton transfer reaction mass spectrometry). Laboratory calibrations were performed for NH_3 measurement and VOCs were selected based on a headspace test of the feeding material (maize silage). Strong interferences of VOCs were observed on NH_3 and greenhouse emissions measured by PAS. Particularly, ethanol, methanol, 1-butanol, 1-propanol and acetic acid were found to have the highest interferences on NH_3, giving empirical relationships in the range of 0.7 to 3.3 ppmv NH_3 per ppmv VOC. A linear response was typically obtained, except for a non-linear relation for VOCs on N_2O concentration. The corrected online NH_3 concentrations measured by PAS in a dairy farm (with empirical relationships 2.1 ± 0.8 and 2.9 ± 1.9 for Location One and Location Two, respectively) were confirmed to be correlated (R^2 = 0.73 and 0.79) to the NH_3 concentration measured simultaneously by the PTR-MS, when the empirical corrections obtained from single VOC tests were applied.

1 Introduction

Measurements of ammonia and greenhouse gas (CH_4, N_2O and CO_2) emissions are gaining increasing attention due to stronger interests on global change and air pollution. Ammonia not only causes serious environmental problems such as soil acidification and pollution of underground water and surface water (van Breemen et al., 1983; Pearson and Stewart, 1993;

45 Erisman et al., 2007), but is also important for fine particle formation (Bouwman et al., 1997;
46 Seinfeld and Pandis, 1997; Pinder et al., 2007). Greenhouse gas emissions, on the other hand,
47 are causing climate change (Thomas et al., 2004; Chadwick et al., 2011). Livestock husbandry
48 was estimated to be responsible for more than 80 % of the ammonia emission in Western Europe
49 (Hutchings et al., 2001; EMEP, 2013) and more than 60% in China (Paulot et al., 2014). In the
50 U.S.A, agriculture accounts for ~90 % of the total ammonia emissions (Aneja et al., 2009).
51 Meanwhile, agriculture accounts for 52 and 84 % of global anthropogenic methane and nitrous
52 oxide emissions (Smith et al., 2008). Accurate measurements of ammonia and greenhouse
53 emissions are therefore vital for reliable emission estimation and thereby the possible reduction
54 of these emissions through various efforts, such as air cleaning with biotrickling filters and air
55 scrubbers (Melse and Van der werf, 2005; De Vries and Melse, 2017). For ammonia
56 measurements, more than 30% difference between different methods has been reported
57 (Scholtens et al., 2004).
58 Infrared photoacoustic spectroscopy (PAS) is a widely-used technique for studies of air
59 emissions especially within agriculture (Osada et al., 1998; Osada and Fukumoto, 2001;
60 Emmenegger et al., 2004; Schilt et al., 2004; Heber et al., 2006; Elia et al., 2006; Blanes-Vidal
61 et al., 2007; Hassouna et al., 2008; Rong et al., 2009; Ngwabie et al., 2011; Cortus et al., 2012;
62 Joo et al., 2013; Wang-Li et al., 2013; Iqbal et al., 2013; Zhao et al., 2016; Ni et al., 2017; Lin
63 et al., 2017). The PAS technique determines the gas concentrations through measuring acoustic
64 signals caused by cell pressure changes when gas absorbs energy from infrared light at a
65 specific wavelength range using an optical filter and a chopper (Iqbal et al., 2013). For example,
66 the Innova 1312 and later versions (Lumasense Technologies, Ballerup, Denmark) uses the PAS

67 principle and was previously verified by the US EPA and recommended by the Air Resources
68 Board in California (CARB, 2000). In principle, this instrument "is capable of measuring
69 almost any gas that absorbs infrared light" (Innova, Lumasense Technology A/S, Denmark).
70 The method is based on nondispersive broadband spectroscopy and selectivity is achieved by
71 using appropriate wavelength filter, with one filter for each targeted trace gas. Innova 1312 and
72 1412 instruments have been used in a large number of tests to measure NH_3, CH_4, CO_2 and N_2O
73 for agricultural applications. Water vapor is also measured to account for the strong absorption
74 of water throughout the infrared spectrum (Christensen, 1990a). Nevertheless, since the infrared
75 spectroscopic method is applied for measuring gas concentrations in PAS, the overlapping of
76 IR spectra with non-targeted gases can introduce significant interferences due to the absorption
77 of infrared light at similar wavelengths. The specificity is limited by the bandwidth of the
78 optical filters. The interferences can be corrected by the instrument software through cross-
79 compensation for all target gases when the instrument is calibrated (Christensen, 1990a;
80 Lumasense, 2012), but understanding and estimation of interferences from non-targeted gases
81 needs to be considered in each specific measurement situation. This is especially important for
82 agricultural applications where the manure and the animal feed may emit various types of gases
83 depending on the management and operations in the animal houses (Hassouna et al., 2013;
84 Moset et al., 2012). Therefore, two key questions exist: (a) what is the magnitude of
85 interferences that can be expected in agricultural environments, and (b) is it possible to quantify
86 and correct interferences in a reasonable way? Until now, the PAS interference has not been
87 well estimated and corrected for, although interferences were previously suspected in livestock
88 facilities (Phillips et al., 2001; Mathot et al., 2007; Ni & Heber, 2008). Flechard et al. (2005)

89 suspected that the N_2O concentration from soil measured by PAS (Innova 1312) was heavily
90 influenced by CO_2 and temperature even when cross-interference compensation was applied;
91 they developed an alternative correction algorithm based on controlled $N_2O/CO_2/H_2O$ ratios
92 under selected temperature. Zhao et al (2012) claimed that the internal cross compensation
93 could eliminate the interferences between target gases, and quantified interferences of non-
94 targeted gas of NH_3 on targeted gases of ethanol, methanol, N_2O, CO_2, and CH_4, however,
95 without giving specific relationships. Iqbal et al. (2013) also demonstrated that a careful
96 calibration could eliminate the internal cross interferences of high water vapor and CO_2
97 concentrations on low concentrations of N_2O at the soil surface by comparison to GC
98 measurements. Nevertheless, tests of interferences by non-targeted VOCs were not included in
99 their study, likely due to the typical low concentrations of VOC in soil (Insam and Seewald,
100 2010). Hassouna et al. (2013) presented a field study on dairy cow buildings, where
101 interferences on NH_3, CH_4 and N_2O were observed. The interferences were suspected to be
102 caused by VOCs (acetic acid, ethanol and 1-propanol) that they measured simultaneously. In
103 their study, two PAS instruments were applied with one of them allocated with optical filters of
104 these VOCs (NH_3 optical filter was included for both PAS). Still, no empirical relationships
105 were given in terms of tested volatile organic compounds, which were typically emitted from
106 feeding materials such as maize silage (Howard et al., 2010; Malkina et al., 2011). The
107 correction of interferences of non-targeted VOCs on NH_3 emission is also essential for the
108 evaluation of emission abatement technologies such as air scrubbers, especially when the inlet
109 VOC concentrations are relatively high. An overestimation of ammonia removal efficiency
110 could easily be obtained since less interference would be expected for the outlet VOCs

111 especially for water-soluble compounds such as the VOCs investigated in this study.

112 In this work, an evaluation of interferences by non-targeted VOCs on targeted NH_3 and
113 greenhouse gas measurements by PAS is presented. The interference on NH_3 was tested by
114 simultaneous application of Proton-transfer-reaction mass spectrometry (PTR-MS), Cavity
115 Ring-Down Spectroscopy (CRDS) and PAS. The experiments were as follows: (1) ammonia
116 laboratory calibration by PAS, PTR-MS and CRDS; (2) VOC selection for testing of
117 interference on ammonia measured by PAS; (3) Effect of VOCs on ammonia and greenhouse
118 emissions measured by the PAS; (4) Field confirmation of interferences of non-targeted VOCs
119 on ammonia measurement and test of potential for data correction.

120 **2 Materials and methods**

121 **2.1 Instrumentation for gas concentrations measurement**

122 In this study, a PTR-MS, a CRDS NH_3 analyzer and a PAS gas analyzer were used to measure
123 trace gas concentrations in air. PTR-MS is a state-of-the-art and widely used technique for
124 highly sensitive online measurements of VOCs (De Gouw and Warneke, 2007; Blake et al.,
125 2009; Yuan et al., 2017). PTR-MS can also measure a few inorganic compounds such as
126 ammonia (at m/z 18) since the proton affinity (204.0 kcal/mol) of ammonia is higher than that
127 of water (165.0 kcal/mol). Since the intrinsic ion at m/z 18 is always formed in the plasma ion
128 source (Norman et al., 2007), ammonia measurements by PTR-MS are routinely corrected for
129 instrumental background contribution. The typical m/z 18 background signal corresponds to a
130 few hundred ppbv of NH_3. The background signal is relatively stable and still allows for NH_3
131 detection limits of 20-50 ppb. For agricultural measurement conditions, concentrations are
132 typically from a few hundred ppb to >10 ppm (e.g., Rong et al., 2009). When total gas

concentration measured by PTR-MS is higher than approximately 10 ppmv, dilution is needed to keep the primary ion signals stable. A high-sensitivity PTR-MS (Ionicon Analytik GmbH, Innsbruck, Austria) was applied for the test of ammonia calibration in the laboratory, effects of non-targeted VOCs on ammonia measurement and field confirmation of interferences of non-targeted VOCs on ammonia measurement. Standard conditions with a total voltage of 600 V in the drift tube were utilized for the PTR-MS. Pressure and temperature in the drift tube were maintained in the range of 2.1-2.2 mbar and at 60 °C, respectively, which gives an E/N ratio of ca. 135 Townsend. The inlet of the PTR-MS is PEEK tubing of 1.2 m length with 0.64 mm inner diameter (ID) and 1.6 mm outer diameter (OD). The inlet flow to the PTR-MS during calibration test and measurements was kept ~150 mL/min. The inlet temperature was maintained at 60 °C. The instrument calibration was performed based on specific reaction rate constants and mass discrimination factors (accuracy better than 12%), as described in our previous study (Liu et al., 2018). Mass calibration was performed before each test, while mass discrimination calibration was performed for every two weeks.

CRDS determines the gas concentration (e.g., NH_3) by measuring the ring-down time of light in the cavity due to absorption by a targeted gas species, which is compared to the ring-down time without any additional absorption due to a targeted gas species. The light source is a laser with tunable wavelength (von Bobrutzki et al., 2010; Picarro, 2017). The very long effective path length of the light in the cavity (e.g., over 20 km for 25 cm cavity) (Picarro, 2017), enables a significantly higher sensitivity compared to conventional absorption spectroscopy (Berden et al., 2000; von Bobrutzki et al., 2010). There is negligible interference from VOCs on CRDS measurements, which makes CRDS ideal to measure NH_3 concentrations in this setting (Kamp

et al., 2019). A G2103 Analyzer (Picarro Inc., Sunnyvale, CA, USA) using CRDS technique was applied in this study for the test of ammonia laboratory calibration and the effect of non-targeted VOCs on ammonia measurement. The accuracy of the CRDS instrument is routinely checked against a certified reference gas as described by Kamp et al (2019). The CRDS analyzer was equipped with two in-line, sub-micron polytetrafluoroethylene (PTFE) particulate matter filters; one at the gas inlet at the back of the analyzer and one at the inlet of the cavity to protect the highly reflective mirrors. The inlet of the CRDS is a PTFE (PTFE) tubing of 1.5 m length with 6.4 mm outer diameter. The optical cavities incorporate precise temperature (±0.005 °C) and pressure (±0.0002 atm) control systems. In this study, both the temperature and pressure of the air sample continuously flowing through the optical cavity are tightly controlled at all times to constant values of 45 °C and 140 Torr, respectively. The measurement interval is around 2 seconds. The CRDS analyzer measured the water vapor simultaneously.

A photoacoustic multi-gas monitor 1312 (Innova, Lumasense Technology A/S, Denmark) was compared with the PTR-MS and the CRDS for ammonia calibration and non-targeted VOCs on ammonia measurement. An infra-red-light source was used for the PAS instrument and the principle for the measurement is as follows. The infrared radiation can interact with a molecule and transfer energy to it if the frequency of the radiation is the same as the frequency of vibration within the molecule. When the molecule absorbs IR light, it vibrates with greater amplitude. This increased activity is short-lived, however, and the excited molecule very quickly transfers its extra energy to other molecules in the vicinity by collision. The increased kinetic energy leads to an increase in the measurement chamber temperature and pressure. A microphone is used to detect the consequently fluctuating pressure. The sample integration time

177 to measure ammonia by PAS was 20 s. The instrument used 6 optical filters for NH_3, CH_4, CO_2,
178 H_2O, N_2O and SF_6. The specifications of the optical filters are shown in Table S1. Water vapor
179 must be included for PAS measurement since the absorbance spectrum of water overlap with
180 other gases such as N_2O and CO_2 thus causing interferences. According to the manufacturer,
181 the Innova 1312 has linear response over a wide dynamic range, with the possibility to make
182 self-calibration (Lumasense, 2012). Before the measurements presented in this study, the
183 supplier calibrated the instrument. During the study the instrument was calibrated based on a
184 certified gas cylinder containing 99.7 (± 10 %) ppmv ammonia (AGA A/S, Copenhagen,
185 Denmark). The interferences between the target gases were therefore supposed to be eliminated
186 through internal cross compensation (Christensen, 1990b; Zhao et al., 2012).

187 **2.2 Experiment 1：laboratory test on ammonia calibration**

188 Instrumental background signals, ammonia calibrations and instrumental response times were
189 characterized for the PAS, PTR-MS and CRDS instruments. For the background measurement,
190 zero air controlled by a mass flow controller (Bronkhorst, Ruurlo, The Netherlands) was
191 supplied, and measurement was performed individually for each instrument. The zero air was
192 supplied from a HiQ zero air station (Linde AG, Munich, Germany). The selected ion
193 measurement mode was used for the PTR-MS with m/z 18 being used for ammonia detection.
194 For the calibration test, a factory-calibrated gas cylinder (AGA A/S, Copenhagen, Denmark)
195 containing 99.7 (± 10 %) ppmv ammonia was used. Mass flow controllers (Bronkhorst, Ruurlo,
196 The Netherlands) were used to dilute the gas from the cylinder with zero air to achieve the
197 desired NH_3 concentration levels (0-11 ppmv). For the test of response decay time, zero air flow
198 was supplied to the instruments at first, then switched to a diluted flow (via 2-levels of mass

199 flow controllers) with ammonia concentration around 5.2 ppmv supplied to all three
200 instruments simultaneously. Subsequently, the ammonia supply was set to zero to test the decay
201 time. Four individual decay time tests were performed for the PAS, to confirm the long decay
202 time of the instrument with low ammonia concentrations (5.2-8.8 ppmv) or high ammonia
203 concentration (99.7 ppmv). For the test of response time for the PAS, two different levels of
204 ammonia concentration were introduced individually to the instrument, to test the dependence
205 of the response time on ammonia concentration.

206 **2.3 Experiment 2: VOCs selection test**

207 A headspace test was performed and VOCs were selected through a PTR-MS measurement as
208 preparation to the interference tests of VOCs on ammonia measured by the PAS. Maize silage
209 is typical feeding material to the cows and silage is generally considered an important source
210 of gaseous VOC in cattle barns. A sample of maize silage was collected from the farm where
211 the field experiment was performed (Skjern, Jutland, Denmark, altitude: 55°59′36.6″, longitude:
212 8°29′53.52″). The silage was then transferred to the laboratory immediately for the headspace
213 test. A clean PTFE container (58×38×43 cm) with two oval holding holes (6×8 cm) on the
214 sides was used for the headspace test. The container was partly open and the silage filled half
215 of the container. A 1-meter 1/4-inch OD PTFE tube was used for the test, with one end placed
216 around 5 cm above the silage, and the other side connected to a T-piece. One side of the T-piece
217 was connected to a 1/8-inch OD PTFE tube (around a half meter) which was connected to the
218 inlet of the PTR-MS. The flow rate of the PTR-MS was kept at 150 mL/min. A zero-air dilution
219 flow (75 mL/min) was supplied to the T-piece to make 1:1 dilution to keep the total
220 concentration below 10 ppmv. The headspace measurement was performed by the PTR-MS in

scan mode, and masses were measured from m/z 21 to m/z 250 with 200 ms for each mass. The selection of VOCs was based on the scan results and relevant literature data on silage VOC, with the following VOCs being selected: ethanol, methanol, acetaldehyde, acetic acid, 2-butanone, acetone, 1-propanol and 1-butanol (Howard et al., 2010; Malkina et al., 2011; Hafner et al., 2013). These 8 selected VOCs were tested for empirical relationships (C_{NH3obs}/C_{VOC}) with respect to contribution to measured NH_3 concentration (C_{NH3obs}). All chemicals were purchased from Sigma-Aldrich with at least analytical grade purity.

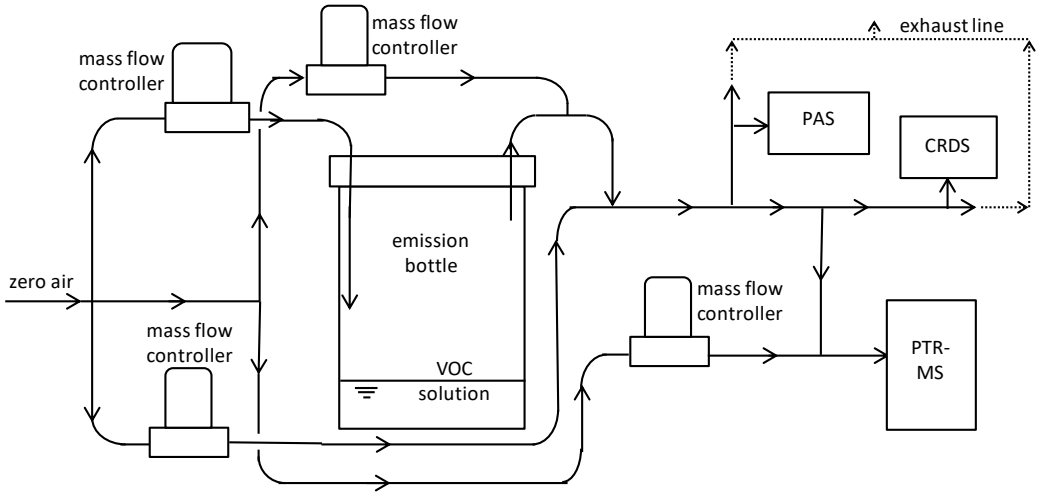

Figure 1. A diagram of the experimental set-up for test of ammonia interference due to VOC.

2.4 Experiment 3: Laboratory test for empirical relationships

The diagram of the setup for the laboratory calibration test is shown in Figure 1. In the setup, a water solution containing the single VOC was purged from the headspace by dry and clean air (or nitrogen for one test on methanol), with flow controlled by a mass flow controller. The air or nitrogen was supplied through a charcoal/silica gel filter. One-liter airtight glass bottles were used for the water solution containing the VOC, and 1/4-inch OD PTFE tube was used in the setup. The purged air flow was diluted with air through a two-step dilution. The flows were

238 adjusted according to the purged VOC concentration and the desired final VOC concentration.
239 The water solution was prepared by using a volume ratio of VOC:Water of 1:5, with purging
240 by clean air controlled by 2 mass flow controllers in order to reach a desired concentration
241 range. For the laboratory test, the diluted air containing VOC was connected to the PAS, the
242 CRDS and the PTR-MS for simultaneous measurements. The overall flow was maintained at a
243 level above the total maximum sampling flow of all three instruments and excess flow was
244 vented through a T-piece. For the PTR-MS measurement, a further dilution by zero air was
245 typically used to keep the total VOC concentrations below 10 ppmv to avoid depletion of the
246 primary ion, H_3O^+. Selected ion measurement mode was applied for the PTR-MS, with an
247 integration time of 2 seconds for the tested VOC mass. During the experiments, the humidity
248 was kept relatively low and stable, with dry clean air used for dilution for all cases, except for
249 one test on methanol, which was also tested under nitrogen condition.

250 **2.5 Experiment 4: Field test for validation of empirical relationships**

251 The field demonstration test for non-targeted VOCs on ammonia measurement by the PAS was
252 performed in the dairy farm mentioned above (Skjern, Jutland, Denmark), where both the PTR-
253 MS and the PAS were measuring continuously over 20 days. The dairy farm housed 360 cows
254 with an average weight of 650 kg. The ventilation system consisted of natural and mechanical
255 partial pit ventilation system (Rong et al., 2015).

256 For the field test, the PAS was combined with a Multiplexer 1309 (Lumasense Technology A/S,
257 Denmark) to measure from several sampling points. The PAS and the PTR-MS were placed in
258 a trailer next to the dairy farm. The PAS sample integration time was 5 s and the flushing time
259 was 20 s. The air concentrations were measured by the PAS sequentially between two selected

locations inside the farm, one location in the pit ventilation, one location outside the farm. PTFE tubes of 20 meters and 8 mm OD were used for the sampling of air. The sampling lines were connected with the channels of the PAS multi-point sampler via continuously running PTFE membrane pumps to ensure constant flushing. VOCs (all VOCs showed in section 2.3 were included together with VOCs reported in previous studies (Malkina et al., 2011; Hafner et al., 2013)) and NH_3 were measured simultaneously by PTR-MS. Measurements were switched between the four measurement sampling lines (connecting to the four locations mentioned above) and the background (outside air beside the trailer) at 8 min intervals via a custom-built switching box. PTFE tubes were used for the PTR-MS sampling lines, which were connected to PTFE sampling lines before the PTFE membranes pumps. The switching box was equipped with a five-port channel selector (Bio-Chem Valve Inc, USA) controlled automatically by 24V outputs from the PTR-MS. A PTFE tube (ID 1 mm) was used to connect the switching box to the inlet sampling line (1-meter PEEK tube with ID 0.64 mm) of the PTR-MS. For selected compounds, calibration was performed for the PTR-MS before the field measurements using permeation tubes and reference gas mixtures. Permeation tubes (VICI Metronics, Inc., Houston, TX, USA) included acetic acid, propanoic acid, butanoic acid, pentanoic acid and 4-methylphenol. Gas mixtures (all 5 ppmv in nitrogen) included hydrogen sulfide (AGA, Copenhagen, Denmark), methanethiol (AGA, Copenhagen, Denmark), and dimethyl sulfide (Air Liquide, Horsens, Denmark). Details regarding the calibration procedures could be found in our previous study, with accuracies within 12% error and in most cases within 8% (Liu et al., 2018). VOC concentrations were determined directly by the PTR-MS, based on estimated reaction rate constants as described by Liu et al. (2018). Standard conditions as described

previously was applied and maintained for the PTR-MS (Feilberg et al., 2010). The mass discrimination was calibrated and adjusted weekly by using a mixture of 14 aromatic compounds between m/z (mass to charge ratio) 79 and 181 (P/N 34423-PI, Restek, Bellefonte, PA). Selected ions were monitored with dwell time between 200 and 2000 ms during each measurement cycle. Masses and dwell time selection was based on ion abundance in full scan mode, relevant literature and experience regarding odorant compounds from dairy buildings as well as from pig houses and pig slurry applications (Shaw et al., 2007; Chung et al., 2009; Liu et al., 2014; Liu et al., 2018).

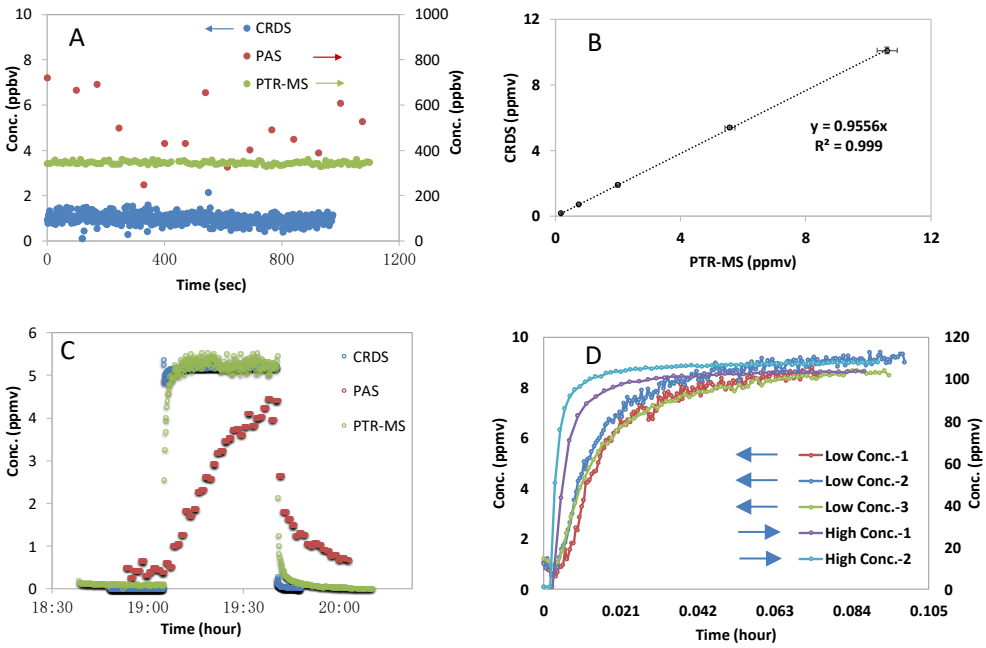

Figure 2. Ammonia test measurements by PAS, PTR-MS and CRDS. A: Background signals measured in ammonia-free air. B: Intercomparison of ammonia concentrations measured by PTR-MS and CRDS. C: Instrumental response of PTR-MS, PAS and CRDS instruments to a rectangular ammonia concentration pulse.; D: Instrumental response of PAS instrument to a stepwise increase in ammonia concentration (low concentration (3 tests; ~8.9 ppmv) and high concentration (2 tests; 99.7 ppmv); Low Conc.-1, Low Conc.-2 and Low Conc.-3 point to the vertical axis on the left, and to the upper horizontal axis; High Conc.-1 and High Conc.-2 point to the vertical axis on the right, and to the lower horizontal axis; High Conc.-2 was tested without the multiplexer). Data in B has been background-subtracted and the linear fits were least square fits without error weighting.

3 Results and discussion

3.1 Experiment 1：laboratory test on ammonia calibration

The instrumental baseline concentrations of ammonia-free zero air measured by PAS, CRDS and PTR-MS, respectively, are shown in Figure 2A, in which a very low background signal was observed for the CRDS instrument (around 1 ppbv) with a detection limit of 0.7 ppbv (3 times the standard deviation of the background). The higher background for ammonia measured from the PTR-MS is caused by the intrinsic formation of NH_4^+ (m/z 18) in the ion source (Norman et al., 2007). Nevertheless, the measured background signals for ammonia by the PTR-MS was very stable and could be subtracted to give a detection limit of 21 ppbv (3 times the standard deviation of the background). Among the three instruments, the PAS gave the highest background signal for ammonia (corresponding to 502±140 ppb), with a detection limit of 421 ppbv (3 times the standard deviation of the background).

For the calibration test of ammonia, the ammonia concentrations simultaneously measured by the CRDS and the PTR-MS is shown in Figure 2B, in which the linearity ($k = 0.96 \pm 0.005$) and high correlation (R^2=0.999) are generally very satisfactory for both instruments. The measured ammonia concentrations also agreed with expected ammonia concentrations from the ammonia reference gas within the uncertainty of 10% provided by the gas supplier.

Table 1. Instruments comparison regarding the specifications for ammonia measurements (SD = standard deviation).

	LOD(3×SD; ppbv)	Upper limit (ppmv)	90% decay time (s)	Measurement time	1σ Accuracy	Possible Interferences
Innova	421(200*)	(-)[A]	1700-4000 (5.2-8.8 ppmv); 450-550 (100 ppmv)	Less than 2 min	Zero Drift: ± 0.25% *	Non-targeted gases with IR spectra Overlapping
PTR-MS	21.5	10[#]	70-80 (5.2 ppmv)	Less than 5 s	(-)	intrinsic ion at m/z 18
Picarro	0.662	>20[&]	4.5-4.7 (5.2 ppmv)	Less than 2 s	(-)	Negligible[&]

* - According to the wall chart given by the producer. https://www.lumasenseinc.com/uploads/Products/Technology_Overview/Technical_Literature_pdf/EN-Lumasense-gas-detection-limits_Wall-Chart.pdf.

A - Not specified by the producer.

- According to the concentration calculation assumption and producer suggestion, total gas concentration should be lower than 10 ppmv, otherwise dilution is needed.

&- According to Kamp et al., 2019.

For the signal decay test, the instrument decay times for ammonia measurements by PAS, CRDS and PTR-MS were measured simultaneously under a static ammonia concentration of 5.2 ppmv. As shown in Figure 2C, ammonia measured by the CRDS showed the shortest decay time while the PAS gave by far the longest decay time. The estimated decay time is shown in Table 1, in which the 90% decay time (time for the concentration to decrease by 90%) for ammonia measured by the CRDS is around 4.5 - 4.7 second, with the 90% decay time from the PTR-MS estimated to be 70 to 80 seconds. The decay time for ammonia measured by the PAS was remarkably longer, with an estimated 90% decay time of around 30 minutes to more than an hour (for four individual tests with ammonia concentration ranged from 5.2 to 8.8 ppmv). When much higher ammonia concentration was used (99.7 ppmv), the 90% decay time measured by the PAS was shorter (450 to 550 seconds). This result is consistent with the response time tests under two levels of input ammonia concentrations (~ 8.9 ppmv and 99.7 ppmv, respectively), with the response time much shorter when the ammonia concentration is

higher, as shown in Figure 2D. Besides, the multiplexer attached to the PAS seemed to increase the response time, as also shown in Figure 2D. However, a very high concentration of about 100 ppmv is not expected in agricultural applications.

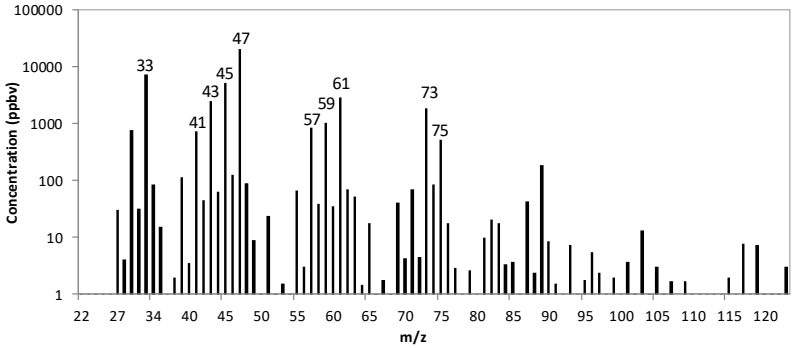

Figure 3. A scan example of the feeding material of silage by using headspace technique measured by the PTR-MS. The m/z 47 is corrected for ethanol fragmentations formed in the PTR-MS through calibration. Selected VOCs for the test in this study were ethanol, methanol, acetaldehyde, acetic acid, 2-butanone, acetone, propanol and butanol.

3.2 Experiment 2: VOCs selection test

The tested VOCs were selected according to a scan test of the headspace from the feeding material of maize silage performed by the PTR-MS, as shown in Figure 3. Due to the fragmentation of ethanol in the PTR-MS measurement (around 10%) (Inomata and Tanimoto, 2009), the concentration corresponding to mass 47 was corrected based on direct calibration under the assumption that mass 47 is solely due to ethanol. The highest peaks of the scan were at masses (m/z): 47, 33, 45, 61, 43, 73, 59, 75, 57 and 41. From the VOCs typically found in the highest concentrations in barns and feeding material (Shaw et al., 2007; Chung et al., 2009; Howard et al., 2010; Malkina et al., 2011; Hafner et al., 2013) and the scan results, a list of VOCs were selected. The following VOCs were selected for the interference tests of non-targeted VOC on ammonia measurement by the PAS: ethanol, methanol, acetaldehyde, acetic acid, 2-butanone, acetone, 1-propanol and 1-butanol. Compounds such as ethanol, methanol,

acetic acid and 1-propanol are typically measured in cattle barns and feeding materials in high concentrations (Shaw et al., 2007; Ngwabie et al., 2008; Howard et al., 2010; Hafner et al., 2013).

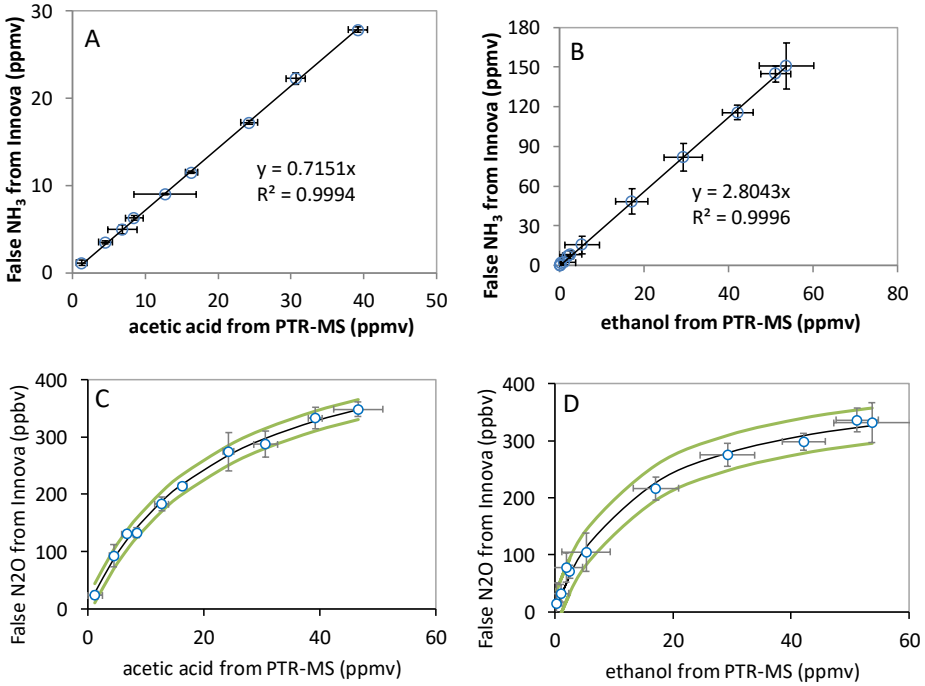

Figure 4. Examples for the interference calibration from non-targeted VOC on NH_3 (A & B) and N_2O (C & D) measured by the PAS. The VOC concentration on the horizontal axis was measured by the PTR-MS, while the NH_3 and N_2O concentrations on vertical axis were from false signals measured meanwhile by the PAS. A: The interference calibration for acetic acid on NH_3; B: The interference calibration for ethanol (corrected for fragments through calibration) on NH_3; C: The interference calibration for ethanol (corrected for fragments through calibration) on N_2O; D: The interference calibration for acetic acid on N_2O. In C & D, the red line indicated the fit curve by equation y=kx/(x+m), and the green and purple curves indicated 95% confidence range. The plotted error bars represent the standard deviations for the measured VOC by the PTR-MS under a selected VOC level (x-axis) and for the measured NH_3/N_2O level by the PAS meanwhile (y-axis). Data were all background-subtracted and the linear fits were least square fits without error weighting.

3.3 Experiment 3: Laboratory test for empirical relationships

The interference of non-targeted VOC on ammonia measurement by the PAS was investigated using single VOC-containing air as inlet measured simultaneously by PAS, PTR-MS and CRDS,

as shown in the setup in Figure 1. An example of the interference test can be seen in Figure S1, where acetic acid was measured simultaneously by the three instruments under various concentration levels. Concentration dependent interference was clear for acetic acid on PAS ammonia measurements.

Table 2. Obtained empirical relationships (slope) describing the functional dependence of the interference in the measurement of the target compound (e.g., NH_3) by PAS on non-targeted VOC concentrations. The value in the brackets indicated the uncertainty (SD of the slope) of the linear fit, except for N_2O where correlation coefficient is shown. N is the number of VOC concentration levels tested for determination of empirical relationships. Nonlinear fit was given for N_2O, where 'x' is measured VOC concentration and 'y' is the false concentration measured by PAS. The concentration range covered for the tested VOC is as follows: ethanol (7 ppbv-58 ppmv); methanol (5 ppbv-45 ppmv); acetic acid (3 ppbv - 48 ppmv); acetaldehyde (8 ppbv-38 ppmv); 2-butanone (3 ppbv - 60 ppmv); acetone (4 ppbv - 48 ppmv); 1-propanol (5 ppbv - 55 ppmv); 1-butanol (6 ppbv - 52 ppmv).

Compound	N	NH_3	CH_4	N_2O (y: ppbv; x: ppmv)	CO_2	SF_6
ethanol	10	2.81(0.02)	1.88(0.01)	y=411x/(x+14) (0.93)	0.40(0.02)	-0.014(0.002)
methanol	9	3.29(0.72)	3.81(0.67)	y=99x/(x+9) (0.78)	0.45(0.17)	-0.15(0.02)
acetic acid	10	0.72x(0.01)	-3.14x(0.08)	y=514x/(x+22) (0.95)	0.39(0.03)	0.31(0.01)
acetaldehyde	4	(-)	-0.85(0.45)	y=317x/(x+31) (0.98)	(-)	0.044(0.021)
2-butanone	4	-0.13x(0.003)	-4.02(0.04)	y=311x/(x+26) (1.00)	-0.61(0.18)	0.23(0.005)
acetone	6	0.02(0.001)	2.10(0.13)	y=104x/(x+4) (0.99)	(-)	0.015(0.001)
1-propanol	5	2.41(0.21)	2.95(0.38)	y=3569x/(x+602) (1.00)	0.25(0.21)	-0.064(0.012)
1-butanol	7	2.66(0.05)	3.07(0.09)	y=807x/(x+73) (0.99)	(-)	-0.061(0.004)
methanol(N_2)	4	1.03(0.31)	1.46(0.22)	(-)	0.35(0.24)	-0.056(0.010)

In principle, establishing empirical correction factors for each specific compound could be used to minimize the interferences of VOCs on the target gas measurements on a specific instrument with the same filter specifications. This requires, however, that VOC concentrations be measured simultaneously by expensive analyzers such as PTR-MS and will in any case result in higher uncertainties due to accumulated uncertainties from multiple interference relationships. Figure 4A & B show two examples of the calibration lines for acetic acid and ethanol, from which an empirical relationship (ER) between the false ammonia concentration

433 and the tested compound could be obtained (ER=0.72 for acetic acid and ER=2.8 for ethanol).
434 A linear response of the ammonia interference was observed for all the tested compounds and
435 they had generally low SD for the slope the linear fits. The ER for ammonia interference by
436 other tested VOCs can be found in Table 2, where ethanol, methanol, 1-propanol and 1-butanol
437 give the highest false signals on ammonia measured by the PAS, with ER of 2.8, 3.3, 2.4 and
438 2.7, respectively. Due to the fact that these compounds are often found in cattle barns and feed
439 silage even in the level of ppmv, especially for ethanol, methanol and 1-propanol (Rabaud et
440 al., 2003; Ngwabie et al., 2008; Howard et al., 2010; Hafner et al., 2013), severe interference
441 on ammonia measured by PAS therefore will occur. While acetic acid gave significant false
442 signals on ammonia (ER=0.72), acetone only showed little interference on ammonia (ER=0.02).
443 Meanwhile, negative false signals were observed for ammonia by 2-butanone (ER=-0.13). Such
444 negative interferences can usually be explained by the internal cross compensation procedure
445 for one target filter (first target filter, such as NH_3 filter) on positive artifacts at another target
446 filter (second target filter, such as CH_4 filter) caused by non-target gas (such as VOC) on the
447 second target filter. This physical explanation was included in a few relevant references such
448 as Zhao et al. (2012). Interestingly, the empirical relationship for false ammonia by methanol
449 in nitrogen matrix is significantly different from that by methanol presented in air matrix
450 (ER=1.03 vs 3.29). This observation is possibly related to the relatively rapid vibrational energy
451 transfer between the VOC and oxygen (Harren et al., 2000). While nitrogen has a vibrational
452 frequency around 2360 cm^{-1}, oxygen has a vibrational frequency of 1554 cm^{-1} with only 170
453 collisions needed to transfer energy to the vibrational mode of O_2 (Lambert, 1977).
454 Besides the interferences on ammonia by the non-targeted VOCs, other target gases also

showed various levels of interferences, as also indicated by previous studies (e.g., Zhao et al., 2012; Hassouna et al., 2013). Because target gases may have more overlap for the infrared spectrum, the primary interference on one target gas caused by the overlap with non-targeted VOCs could therefore influence and cause secondary interference on other target gases (Zhao et al., 2012; Adamsen, 2018). Still, in theory, empirical relationships could be obtained for the interfered gases by the tested VOCs. Specifically, for the interference on methane by non-targeted methanol, 1-butanol, 1-propanol, acetone and ethanol showed positive false signals (ER=3.8, 3.1, 3.0, 2.1, 1.9, respectively). 2-butanone, acetic acid and acetaldehyde showed negative false signals to methane, with ER equal to -4.02, -3.14 and -0.85, respectively. An explanation for the negative false signals could be that absorption takes place in the band for H_2O correction (Adamsen, 2018). All interferences on methane are shown in Table 2. For methanol in nitrogen, the calibration showed a significant difference compared to air (ER=1.46 vs. 3.81).

Meanwhile, the non-targeted VOC also caused false signals on nitrous oxide signals, with a much lower level of interference. Furthermore, the calibrations of the nitrous oxide interference by the non-targeted VOCs seemed not to be following linear relationships. For examples, Figure 4C & D showed the false signals of nitrous oxide caused by ethanol and acetic acid. A non-linear relationship exists between nitrous oxide interference and VOC concentration. The curves could be well fitted to the non-linear equation of $y = kx/(x+m)$, where k represents the maximum interference on nitrous oxide by the single VOC, m represents the half-saturation constant indicating the level higher at which the VOC concentration could cause half of the maximum interference on nitrous oxide. As shown in Table 2, all tested VOCs showed positive

477 non-linear interference to the nitrous oxide signals, and 1-butanol showed the highest maximum
478 interference on nitrous oxide. Interestingly, no interference was observed for nitrous oxide
479 when methanol was presented in a nitrogen matrix, while a relatively lower level of interference
480 by methanol was observed for nitrous oxide when presented in atmospheric air.
481 Furthermore, some of the tested VOCs also caused interference on carbon dioxide measured by
482 the PAS. The background of carbon dioxide was considered as unchanged during the
483 interference tests. While methanol, ethanol, acetic acid and 1-propanol caused positive false
484 signals for carbon dioxide measured by the PAS (ER = 0.45, 0.40, 0.39, 0.25, respectively), 2-
485 butanone caused negative false signals with ER = -0.61 (Table 2). Other tested VOCs, including
486 acetone, acetaldehyde and 1-butanol, did not show interferences on carbon dioxide measured
487 by the PAS. This is likely because no overlap of the gas infrared adsorption spectra exists
488 between these VOCs and carbon dioxide. As expected, methanol in nitrogen also caused
489 interference on carbon dioxide (ER =0.35) slightly lower than methanol in air.
490 Besides, SF_6 measurements were interfered by the tested non-targeted VOC, with lower
491 empirical relationship obtained compared to NH_3, CH_4, N_2O and CO_2. Acetic acid and 2-
492 butanone caused the highest interferences on SF_6, with ER of 0.31 and 0.23, respectively. Other
493 tested VOCs caused significantly less interference on SF_6, among which methanol gave the
494 highest negative ER of -0.15. Again, the methanol in nitrogen gave a significantly lower level
495 of interference on SF_6 compared to methanol in air (ER = -0.056 vs -0.15).
496 Overall, the tested non-target VOCs in this study caused significant interference on target gases,
497 of which ammonia and methane were influenced to the largest degree. Even though less
498 interference was observed for nitrous oxide, this could still cause problems due to the typically

low concentration level of this compound in e.g. livestock facilities or soil (Iqbal et al., 2013; Rong et al., 2014).

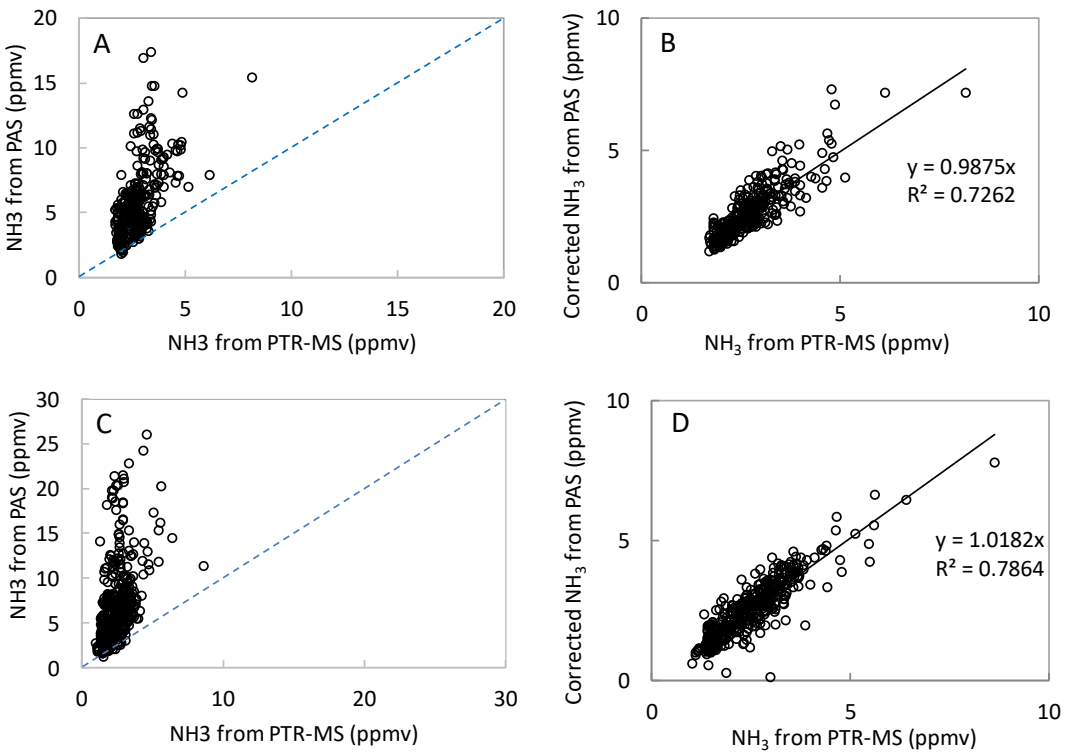

Figure 5. NH_3 concentrations measured by the PAS (vertical axis) and by the PTR-MS (horizontal axis) in the field measurement from Location One before the correction by the tested non-targeted VOCs (A) and after the correction by the tested non-targeted VOCs (B), and from Location Two before the correction by the tested non-targeted VOCs (C) and after the correction by the tested non-targeted VOCs (D). Data from B and D were background corrected and the linear fits were least square fits without error weighting.

3.4 Experiment 4: Field test for validation of empirical relationships

During the field test in the dairy barn, the ammonia measurements by PAS and PTR-MS were compared to each other for one location in the pit and two locations (Location One and Location

Two) in the barn. Figure S2 shows ammonia concentration measured by PAS and PTR-MS at the pit ventilation. In the pit ventilation, low concentrations of VOCs were generally obtained and relatively high concentrations of ammonia were observed for both instruments. Thus, no significant interferences were observed for ammonia measured by the PAS, and ammonia measurements by PAS and PTR-MS showed a good agreement as shown in Figure S2. However, for the two measurement points inside the barn, significantly higher ammonia concentrations were obtained from PAS compared to the concentrations measured by PTR-MS (Figure 5 A & C). Table S2 showed the percentage for each range of ratio of PAS/PTR-MS concentrations for the data shown in Figure 5 A & C, where ratio of PAS/PTR-MS concentrations mostly within 1-4. The higher ammonia concentration observed for the PAS measurement is ascribed to interferences from VOCs, some of which had high concentrations, especially for ethanol as shown in Table 3. The relation between the ammonia concentrations measured by PAS and the ethanol concentrations measured by PTR-MS were highly correlated for both measurement locations, with slopes close to 3 (3.0 and 3.1; see Figure S3). These two numbers are generally close to the empirical relationship obtained for ethanol (ER = 2.8). The empirical relationships obtained in 'Experiment 3' were used for data correction of ammonia measurement by PAS since the instrument configurations were kept the same. Thus, the interference of the VOCs on ammonia measurement by PAS could be estimated from the empirical relationships obtained in 'Experiment 3' and used to correct the ammonia data. Figure 5B & D show the corrected ammonia concentrations measured by PAS by using the empirical relationships, together with the measured ammonia concentration by the PTR-MS for both measurement locations. The corrected ammonia concentrations from the PAS are generally in good agreement with the

559 ammonia concentration measured by the PTR-MS, with slopes close to 1 (0.99 and 1.02). It
560 should be noted that although the empirical relationships were obtained for single VOC
561 interferences on ammonia measurement by PAS, they were treated as being additive under field
562 conditions where multiple VOCs presented. Ethanol dominated the VOC composition in
563 general, but other types of VOC also contribute significantly. The average ratio of ethanol
564 concentration to the sum of the 8 VOCs (tested in the lab with obtained empirical relationships)
565 was 0.64 (±0.11) for Location Two in the field study. This single application suggests that the
566 interference is close to additive, but further investigation is needed to confirm this finding. The
567 cattle barn experiment validated that correction from major VOCs is necessary for reliable PAS
568 measurements. In principle, it is possible to estimate the interference on NH3 measured by PAS
569 measurements in field applications. However, it should be noted that a lot of redundant work is
570 needed to make this correction if only NH_3 concentration is measured since the concentrations
571 of several VOCs need to be known to achieve a proper correction.

572

573 **Table 3.** Average concentrations (±standard deviation) of selected VOCs during the field test in the
574 dairy cattle barn for the two sampling locations 1 & 2, both of which are located inside the barn. The
575 standard deviation applies to the mean values.

Compound	Concentrations (ppbv)	
	Location 1	Location 2
ethanol	1421±946	1622±1355
methanol	237.2±150.2	241.1±192.3
acetic acid	57.2±41.3	69.4±61.6
acetaldehyde	98.8±81.2	92.2±83.7
2-butanone	19.1±11.0	17.2±13.1
acetone	77.9±30.2	52.1±24.9
1-propanol	71.0±45.2	71.8±67.7
1-butanol	22.2±10.1	16.3±11.8
hydrogen sulfide	12.1±9.7	11.3±8.4
trimethylamine	8.6±3.5	5.7±3.1
dimethyl sulfide	15.1±9.2	14.3±9.8
4-methylphenol	5.2±2.1	3.8±2.2

576

4 Conclusions

When measuring NH_3 and greenhouse gas emissions (CH_4, N_2O and CO_2) by PAS, non-target VOCs may interfere significantly with the target gases causing inaccurate results. To confirm and determine the magnitude of interferences, experiments have been conducted by simultaneously using a PAS and a PTR-MS. Results from these experiments provide useful guidelines concerning interferences caused by non-targeted VOCs. The results demonstrate that ethanol, methanol, 1-butanol, 1-propanol and acetic acid are causing the most significant interferences on NH_3 measured by PAS. A field test in a cattle barn validated the interference caused by VOCs on NH_3 measurement by PAS by simultaneously measuring VOCs with PTR-MS.

Code and data availability. Data and code are available upon request to the corresponding author.

Supplement. The supplementary information is available free of charge at DOI: .

Author contributions. DL, LR and AF designed the setup for the experiments performed; LR, JK and AC contributed to setting up and conducting experiments and acquiring data; DL, AF, JK, XK and APA contributed to writing the manuscript, data interpretation and data analysis; LR, AF and JK assisted in data analysis and manuscript editing.

Competing interests. The authors declare that they have no conflicts of interest.

Acknowledgements. Part of this work was supported by National Natural Science Fund of China (No. 31672468) and Thousand Talents Program (Youth Project 2016).

References

Adamsen, A.P. Measurement of climate gases from livestock barns with infrared photo-acoustic spectrometry (In Danish: Måling af klimagasser fra stalde med infrarød fotoakustisk spektrometri), Technical Report, SEGES, December, 2018.

Aneja, V. P., Schlesinger, W. H., and Erisman, J. W.: Effects of agriculture upon the air quality and climate: research, policy, and regulations, Environ. Sci. Technol., 43, 4234–4240, https://doi.org/10.1021/es8024403, 2009.

Angela, E., Di, F. C., Mario, L. P., and Gaetano, S.: Photoacoustic Spectroscopy with Quantum Cascade Lasers for Trace Gas Detection, Sensors-Basel, 6, 1411–1419, https://doi.org/10.3390/s6101411, 2006.

Inomata S., Tanimoto H.: A deuterium-labeling study on the reproduction of hydronium ions in the PTR-MS detection of ethanol, Int. J. Mass Spectrom., 285, 95-99, http://doi.org/ 10.1016/j.ijms.2009.05.001,2009.

Berden, G., Peeters, R., and Meijer, G.: Cavity ring-down spectroscopy: Experimental schemes and applications, Int. Rev. Phys. Chem., 19, 565–607, https://doi.org/10.1080/014423500750040627, 2000.

Blake, R. S., Monks, P. S., and Ellis, A. M.: Proton-transfer reaction mass spectrometry, Chem. Rev., 109, 861–896, https://doi.org/10.1002/chin.200923275, 2009.

621 Blanes-Vidal, V., Topper, P. A., and Wheeler, E. F.: Validation of ammonia emissions from dairy
622 cow manure estimated with a non-steady-state, recirculation flux chamber with whole-
623 building emissions, T. ASABE, 50, 633–640, https://doi.org/10.13031/2013.22652, 2007.
624 Bouwman, A. F., Lee, D. S., Asman, W. A. H., Dentener, F. J., Van, D. H. K. W., and Olivier, J.
625 G. J.: A global high-resolution emission inventory for ammonia, Global Biogeochem. Cy.,
626 11, 561–587, https://doi.org/10.1029/97GB02266, 1997.
627 California Air Resources Board (CARB).: Manufacturer Notification. Mail-Out #MSO 2000-
628 08, CARB: Sacramento, CA, USA, Available online:
629 http://www.arb.ca.gov/msprog/mailouts/ mso0008/mso0008.pdf, 2000.
630 Chadwick, D., Sommer, S., Thorman, R., Fangueiro, D., Cardenas, L., Amon, B., and
631 Misselbrook, T.: Manure management: Implications for greenhouse gas emissions, Anim.
632 Feed Sci. Tech., 166-167, 514–531, https://doi.org/10.1016/j.anifeedsci.2011.04.036, 2011.
633 Christensen J. The Brüel&Kjær Photoacoustic Transducer System and its Physical Properties.
634 Brüel&Kjær Technical Review, 1, 1990a.
635 Christensen J. Optical filters and their use with the type 1302 type 1306 phtoacoustic gas
636 monitors. Brüel&Kjær Technical Review, 2, 1990b.
637 Chung, M.Y., Beene, M., Ashkan, S., Krauter, C., and Hasson, A.S.: Evaluation of non-enteric
638 sources of non-methane volatile organic compound (NMVOC) emissions from dairies,
639 Atmos. Environ., 44, 786–794, https://doi.org/10.1016/j.atmosenv.2009.11.033, 2009.
640 Cortus E.L., Jacobson L.D., Hetchler B.P., and Heber A.J.: Emission monitoring methodology
641 at a NAEMS dairy site, with an assessment of the uncertainty of measured ventilation rates,
642 ASABE - 9th International Livestock Environment Symposium, 583-590,

https://doi.org/10.13031/2013.41578, 2012.

De Gouw J., and Warneke C.: Measurements of volatile organic compounds in the earth's atmosphere using proton-transfer-reaction mass spectrometry, Mass Spectrom. Rev., 26, 223–257, https://doi.org/10.1002/mas.20119, 2007.

EMEP, Agency: EMEP/EEA air pollutant emission inventory guidebook - 2013. *Luxembourg: Publications Office of the European Union,* 3B: Manure management, https://www.eea.europa.eu/publications/emep-eea-guidebook-2013/part-b-sectoral-guidance-chapters/4-agriculture/3-b-manure-management/view, 2013.

Emmenegger, L., Mohn J., Sigrist M., Marinov D., Steinemann U., Zumsteg F., and Meier M.: Measurement of ammonia emissions using various techniques in a comparative tunnel study, Int. J. Environ. Pollut., 22, 326–341, https://doi.org/10.1504/IJEP.2004.005547, 2004.

Erisman, J. W., Bleeker, A., Galloway, J., and Sutton, M. S.: Reduced nitrogen in ecology and the environment, Environ. Pollut., 150, 140–149, https://doi.org/10.1016/j.envpol.2007.06.033, 2007.

Feilberg A., Liu D., Adamsen A.P.S., Hansen M.J., and Jonassen K.E.N.: Odorant emissions from intensive pig production measured by online proton-transfer-reaction mass spectrometry, Environ. Sci. Technol., 44, 5894–5900, https://doi.org/10.1021/es100483s, 2010.

Fle´chard, C. R., Neftel, A., Jocher, M., Ammann, C., and Fuhrer, J.: Bi-directional soil/atmosphere N2O exchange over two mown grassland systems with contrasting management practices, Global Change Biol., 11, 2114–2127, https://doi.org/10.1111/j.1365-2486.2005.01056.x, 2010.

Hafner S.D., Howard C., Muck R.E., Franco R.B., Montes F., Green P.G., Mitloehner F., Trabue, S.L., and Rotz C.A.: Emission of volatile organic compounds from silage: Compounds, sources, and implications, Atmos. Environ., 77, 827–839, https://doi.org/10.1016/j.atmosenv.2013.04.076, 2013.

Hafner, S. D., Montes, F., Rotz, C. A., and Mitloehner, F.: Ethanol emission from loose corn silage and exposed silage particles. Atmos. Environ., 44, 4172–4180, https://doi.org/10.1016/j.atmosenv.2010.07.029, 2010.

Harren F.J.M., Cotti G., Oomens J., and Hekkert S.L.: Photoacoustic Spectroscopy in Trace Gas Monitoring, in Encyclopedia of Analytical Chemistry, R.A. Meyers (Ed.), 2203–2226, ©JohnWiley & Sons Ltd, Chichester, 2000.

Hassouna, M., Espagnol, S., Robin, P., Paillat, J. M., Levasseur, P., and Li, Y.: Monitoring NH3, N2O, CO2 and CH4 emissions during pig solid manure storage and effect of turning, Compost Sci. Util., 16, 267–274, https://doi.org/10.1080/1065657X.2008.10702388, 2008.

Hassouna, M., Robin, P., Charpiot, A., Edouard, N., and Méda, B.: Infrared photoacoustic spectroscopy in animal houses: Effect of non-compensated interferences on ammonia, nitrous oxide and methane air concentrations, Biosyst. Eng., 114, 318–326, https://doi.org/10.1016/j.biosystemseng.2012.12.011, 2013.

Heber A.J., Ni J.-Q., Lim T.T., Tao P.-C., Schmidt A.M., Koziel J.A., Beasley D.B., Hoff, S.J., Nicolai, R.E., Jacobson, L.D., and Zhang Y.: Quality assured measurements of animal building emissions: Gas concentrations, J. Air Waste Manage., 56, 1472–1483, https://doi.org/10.1080/10473289.2006.10465680, 2006.

Heyden, C. V. D., Brusselman, E., Volcke, E. I. P., and Demeyer, P.: Continuous measurements

687 of ammonia, nitrous oxide and methane from air scrubbers at pig housing facilities, J.
688 Environ. Manage., 181, 163–171, https://doi.org/10.1016/j.jenvman.2016.06.006, 2016.
689 Howard, C. J., Kumar, A., Malkina, I., Mitloehner, F., Green, P. G., Flocchini, R. G., and
690 Kleeman, M. J.: Reactive organic gas emissions from livestock feed contribute significantly
691 to ozone production in central California, Environ. Sci. Technol., 44, 2309–2314,
692 https://doi.org/ 10.1021/es902864u, 2010.
693 Hutchings, N. J., Sommer, S. G., Andersen, J. M., and Asman, W. A. H.: A detailed ammonia
694 emission inventory for Denmark, Atmos. Environ., 35, 1959–1968,
695 https://doi.org/10.1016/S1352-2310(00)00542-2, 2001.
696 Insam, H., and Seewald, M. S. A.: Volatile organic compounds (VOCs) in soils, Biol. Fert. Soils,
697 46, 199–213, https://doi.org/10.1007/s00374-010-0442-3, 2010.
698 Iqbal, J., Castellano, M.J., and Parkin, T.B.: Evaluation of photoacoustic infrared spectroscopy
699 for simultaneous measurement of N2O and CO2 gas concentrations and fluxes at the soil
700 surface, Global Change Biol., 19, 327–336, https://doi.org/10.1111/gcb.12021, 2013.
701 Jie, D. F., Wei, X., Zhou, H. L., Pan, J. M., and Ying, Y. B.: Research progress on interference
702 in the detection of pollutant gases and improving technology in livestock farms: A review,
703 Appl. Spectrosc. Rev., 52,101–122, https://doi.org/10.1080/05704928.2016.1208213, 2016.
704 Joo H.S., Ndegwa P.M., Neerackal G.M., Wang X., and Harrison J.H.: Effects of manure
705 managements on ammonia, hydrogen sulfide and greenhouse gases emissions from the
706 naturally ventilated dairy barn, ASABE, 2 , 1302-1311,
707 https://doi.org/10.13031/aim.20131593447, 2013.
708 Kamp, J.N., Chowdhury, A., Adamsen, A.P.S., Feilberg, A.: Negligible influence of livestock

709 contaminants and sampling system on ammonia measurements with cavity ring-down
710 spectroscopy. Atmos. Meas. Tech., 12, 2837–2850, https://doi.org/10.5194/amt-12-2837-
711 2019, 2019.
712 Lambert J.D.: Vibrational and Rotational Relaxation in Gases, Clarendon Press, Oxford, **1977**.
713 Lin, X., Zhang, R., Jiang, S., El-Mashad, H., and Xin, H.: Emissions of ammonia, carbon
714 dioxide and particulate matter from cage-free layer houses in California, Atmos. Environ.,
715 152, 246–255, https://doi.org/10.1016/j.atmosenv.2016.12.018, 2017.
716 Liu D., Lokke M.M., Leegaard Riis A., Mortensen K., and Feilberg A.: Evaluation of clay
717 aggregate biotrickling filters for treatment of gaseous emissions from intensive pig
718 production, J. Environ. Manage., 136, 1–8, https://doi.org/10.1016/j.jenvman.2014.01.023,
719 2014.
720 Liu, D., Nyord, T., Rong, L., and Feilberg, A.: Real-time quantification of emissions of volatile
721 organic compounds from land spreading of pig slurry measured by PTR-MS and wind
722 tunnels, Sci. Total. Environ., 639, 1079–1087,
723 https://doi.org/10.1016/j.scitotenv.2018.05.149, 2018.
724 Lumasense.: Photoacoustic Gas Monitor - INNOVA 1412i.
725 http://www.lumasenseinc.com/FR/produits/gas-sensing/gas-monitoring-
726 instruments/photoacoustic-spectroscopy-pas/photoacoustic-gas-monitor-innova-1412i/.
727 Accessed 18th November, 2018.
728 Malkina, I.L., Kumar, A., Green, P.G., and Mitloehner, F.M.: Identification and quantitation of
729 volatile organic compounds emitted from dairy silages and other feedstuffs, J. Environ. Qual.,
730 40, 28, https://doi.org/10.2134/jeq2010.0302, 2011.

731 Mathot, M., Decruyenaere, V., Lambert, R., Stilmant, D. Emissions de CH_4, N_2O et NH_3 en
732 e´tables et lors du stockage des engrais de ferme de ge´nisses Blanc Bleu Belge. Paper
733 presented at the 14e`me Journe´es 3R, Paris, 2007.
734 Melse, R. W., and Werf, A. W. V. D.: Biofiltration for mitigation of methane emission from
735 animal husbandry, Environ. Sci. Technol., 39, 5460, https://doi.org/10.1021/es048048q,
736 2005.
737 Moset, V., Cambra-López, M., Estellés, F., Torres, A. G., and Cerisuelo, A.: Evolution of
738 chemical composition and gas emissions from aged pig slurry during outdoor storage with
739 and without prior solid separation, Biosyst. Eng., 111, 2–10,
740 https://doi.org/10.1016/j.biosystemseng.2011.10.001, 2012.
741 Ngwabie, N. M., Jeppsson, K. H., Gustafsson, G., and Nimmermark, S.: Effects of animal
742 activity and air temperature on methane and ammonia emissions from a naturally ventilated
743 building for dairy cows, Atmos. Environ., 45, 6760–6768,
744 https://doi.org/10.1016/j.atmosenv.2011.08.027, 2011.
745 Ngwabie, N.M., Schade, G.W., Custer, T.G., Linke, S., and Hinz, T.: Abundances and flux
746 estimates of volatile organic compounds from a dairy cowshed in Germany, J. Environ. Qual.,
747 37, 565–573, https://doi.org/10.2134/jeq2006.0417, 2008.
748 Ni, J. Q., and Heber, A. J.: Sampling and Measurement of Ammonia at Animal Facilities, Adv.
749 Agron., 98, 201–269, https:// doi.org/10.1016/s0065-2113(08)00204-6, 2008.
750 Ni, J. Q., Diehl, C. A., Chai, L., Chen, Y., Heber, A. J., Lim, T. T., and Bogan, B. W.: Factors
751 and characteristics of ammonia, hydrogen sulfide, carbon dioxide, and particulate matter
752 emissions from two manure-belt layer hen houses, Atmos. Environ., 156,

https://doi.org/10.1016/j.atmosenv.2017.02.033, 2017.

Norman, M., Hansel, A., and Wisthaler, A.: O2+ as reagent ion in the PTR-MS instrument: Detection of gas-phase ammonia, Int. J. Mass Spectrom., 265, 382–387, https://doi.org/10.1016/j.ijms.2007.06.010, 2007.

Osada, T., and Fukumoto, Y.: Development of a new dynamic chamber system for measuring harmful gas emissions from composting livestock waste, Water Sci. Technol., 44, 79–86, https://doi.org/10.2166/wst.2001.0513, 2001.

Osada, T., Rom H.B., and Dahl P.: Continuous measurement of nitrous oxide and methane emission in pig units by infrared photoacoustic detection, T. ASAE, 41, 1109–1114, https://doi.org/10.13031/2013.17256, 1998.

Paulot, F., Jacob, D. J., Pinder, R. W., Bash, J. O., Travis, K., and Henze, D. K.: Ammonia emissions in the United States, European Union, and China derived by high - resolution inversion of ammonium wet deposition data: Interpretation with a new agricultural emissions inventory (MASAGE_NH3), J. Geophys. Res., 119, 4343–4364, https://doi.org/10.1002/2013JD021130, 2015.

Pearson, J., and Stewart, G. R.: The deposition of atmospheric ammonia and its effects on plants, New Phytol., 125, 283–305, https://doi.org/10.1111/j.1469-8137.1993.tb03882.x, 1993.

Picarro.: Technology: Cavity Ring-Down Spectroscopy (CRDS), Link: https://www.picarro.com/technology/cavity_ring_down_spectroscopy. Accessed 12th May, 2018.

Phillips, V. R., Lee, D. S., Scholtens, R., Garland, J. A., and Sneath, R. W.: SE—Structures and Environment : A Review of Methods for measuring Emission Rates of Ammonia from

775 Livestock Buildings and Slurry or Manure Stores, Part 2: monitoring Flux Rates,
776 Concentrations and Airflow Rates, J. Agr. Eng. Res., 78, 1–14,
777 https://doi.org/10.1006/jaer.2000.0618, 2001.
778 Pinder, R. W., Adams, P. J., and Pandis, S. N.: Ammonia emission controls as a cost-effective
779 strategy for reducing atmospheric particulate matter in the Eastern United States, Environ.
780 Sci. Technol., 41, 380–6, https://doi.org/10.1021/es060379a, 2007.
781 Rabaud, N.E., Ebeler, S.E., Ashbaugh, L.L., and Flocchini, R.G.: Characterization and
782 quantification of odorous and non-odorous volatile organic compounds near a commercial
783 dairy in California, Atmos. Environ., 37, 933–940, https://doi.org/10.1016/S1352-
784 2310(02)00970-6, 2003.
785 Rong L., Liu D., Pedersen E.F., and Zhang G.: Effect of climate parameters on air exchange
786 rate and ammonia and methane emissions from a hybrid ventilated dairy cow building, Energ.
787 Buildings, 82, 632–643, https://doi.org/10.1016/j.enbuild.2014.07.089, 2014.
788 Rong L., Liu D., Pedersen E.F., Zhang G. The effect of wind speed and direction and
789 surrounding maizeon hybrid ventilation in a dairy cow building in Denmark. Energy and
790 Buildings, 86, 25-34, https://doi.org/ 10.1016/j.enbuild.2014.10.016, 2015.
791 Rong, L., Nielsen, P. V., and Zhang, G. Q.: Effects of airflow and liquid temperature on
792 ammonia mass transfer above an emission surface: experimental study on emission rate,
793 Bioresource Technol., 100, 4654–4661, https://doi.org/10.1016/j.biortech.2009.05.003, 2009.
794 Schilt, S., Thévenaz, L., Niklès, M., Emmenegger, L., and Hüglin, C.: Ammonia monitoring at
795 trace level using photoacoustic spectroscopy in industrial and environmental applications,
796 Spectrochim. Acta. A, 60, 3259–3268, https://doi.org/10.1016/j.saa.2003.11.032, 2004.

797 Scholtens, R., Jones, C. J. D. M., Lee, D. S., and Phillips, V. R.: Measuring ammonia emission
798 rates from livestock buildings and manure stores—part 1: development and validation of
799 external tracer ratio, internal tracer ratio and passive flux sampling methods, Atmos. Environ.,
800 38, 3003–3015, https://doi.org/10.1016/j.atmosenv.2004.02.030, 2004.
801 Seinfeld, J.H.; and Pandis, S.N.: Atmospheric Chemistry and Physics: From Air Pollution to
802 Climate Change, Wiley-VCH: New York. 1326 pp., ISBN 0-471-17815-2, 1997.
803 Shaw, S.L., Mitloehner, F.M., Jackson, W., Depeters, E.J., Fadel, J.G., Robinson, P.H.,
804 Holzinger, R., and Goldstein, A.H.: Volatile organic compound emissions from dairy cows
805 and their waste as measured by proton-transfer-reaction mass spectrometry, Environ. Sci.
806 Technol., 41, 1310–1316, https://doi.org/10.1021/es061475e, 2007.
807 Smith, P., Martino, D., Cai, Z., Gwary, D., Janzen, H., Kumar, P., Mccarl, B., Ogle, S., O'Mara,
808 F., and Rice, C.: Greenhouse gas mitigation in agriculture, Philos. T. R. Soc. B, 363, 789–
809 813, https://doi.org/10.1098/rstb.2007.2184, 2008.
810 Thomas, C. D., Cameron, A., Green, R. E., Bakkenes, M., Beaumont, L. J., Collingham, Y. C.,
811 Erasmus, B. F., De Siqueira, M. F., Grainger, A., and Hannah, L.: Extinction risk from climate
812 change, Nat., 427, 145–148, https://doi.org/10.1038/nature02121, 2004.
813 Van Breemen, N., Mulder, J., and Driscoll, C. T.: Acidification and alkalinization of soils, Plant
814 Soil, 75, 283–308, https://doi.org/10.1007/BF02369968, 1983.
815 Von Bobrutzki, K., Braban, C.F., Famulari, D., Jones, S.K., Blackall, T., Smith, T.E.L., Blom,
816 M., Coe, H., Gallagher, M., Ghalaieny, M., McGillen, M.R., Percival, C.J., Whitehead, J.D.,
817 Ellis, R., Murphy, J., Mohacsi, A., Pogany, A., Junninen, H., Rantanen, S., Sutton, M.A., and
818 Nemitz, E.: Field inter-comparison of eleven atmospheric ammonia measurement techniques,

819 Atmos. Meas. Tech+., 3, 91–112, https://doi.org/10.5194/amt-3-91-2010, 2010.
820 Vries, J. W. D., and Melse, R. W.: Comparing environmental impact of air scrubbers for
821 ammonia abatement at pig houses: A life cycle assessment, Biosyst. Eng., 161, 53–61,
822 https://doi.org/10.1016/j.biosystemseng.2017.06.010, 2017.
823 Wang-Li L., Li Q.-F., Chai L., Cortus E.L., Wang K., Kilic I., Bogan B.W., Ni J.-Q., and Heber
824 A.J.: The national air emissions monitoring study's Southeast Layer Site: Part III. Ammonia
825 concentrations and emissions, T. ASABE, 56, 1185–1197, https://
826 doi.org/10.13031/trans.56.9673, 2013.
827 Yuan, B., Koss, A.R., Warneke, C., Coggon, M., Sekimoto, K., and de Gouw, J.A.: Proton-
828 Transfer-Reaction Mass Spectrometry: Applications in Atmospheric Sciences, Chem. Rev.,
829 117, 13187–13229, https://doi.org/10.1021/acs.chemrev.7b00325, 2017.
830 Zhao, L., Hadlocon, L. J. S., Manuzon, R. B., Darr, M. J., Keener, H. M., Heber, A. J., and Ni,
831 J.: Ammonia concentrations and emission rates at a commercial poultry manure composting
832 facility, Biosyst. Eng., 150, 69–78, https://doi.org/10.1016/j.biosystemseng.2016.07.006,
833 2016.
834 Zhao, Y., Pan, Y., Rutherford, J., and Mitloehner, F. M.: Estimation of the Interference in Multi-
835 Gas Measurements Using Infrared Photoacoustic Analyzers, Atmos., 3, 246–265,
836 https://doi.org/10.3390/atmos3020246, 2012.